Shear bands due to heat flux prescribed at boundaries

R.C. Batra *, Z.G. Wei

Department of Engineering Science and Mechanics, MC 0219, Virginia Polytechnic Institute and State University, Blacksburg, VA 24061, USA

R.C. Batra dedicates this work to professor Akhtar S. Khan on his 60th birthday

Abstract

We analyze the initiation and development of a shear band in a thermo-elasto-viscoplastic body deformed in simple shear by tangential velocity and heat flux prescribed at the outer bounding surfaces. Unlike previous studies no defect is introduced to initiate a shear band. The prescribed heat flux acts as a defect, and the shear band initiation time depends upon it. © 2005 Elsevier Ltd. All rights reserved.

Keywords: Thermomechanical deformations; Finite strains; Inertia effects; Deformation localization; Finite element solution

1. Introduction

This work is motivated by high speed manufacturing processes such as extrusion, punching, machining and friction stir welding. Aukrust and Lazghab (2000) found that during extrusion of aluminum alloy AA6082 at 0.175 m/s deformations localized into a thin layer 250 μm wide adjacent to the die wall. Frictional forces between

---
* Corresponding author. Tel.: +1 540 231 6051; fax: +1 540 231 4574.
 E-mail addresses: rbatra@vt.edu (R.C. Batra), zwei@vt.edu (Z.G. Wei).

the work-piece and the die wall generate considerable heat. A similar situation occurs during the punching of a hole in a plate where frictional forces between the work-piece and the die and the accompanying high strain rates can generate significant heat flux; e.g. see Moss (1981), Zener and Hollomon (1944). In friction stir welding (e.g. see Seidel and Reynolds (2001), Schneider and Nunes (2004)) the tool rotating at a very high speed has a small diameter entry probe and a concentric large diameter shoulder to compress the two plates to be welded. The tool translates at a uniform speed. Heat due to friction generates a column of molten material undergoing essentially Couette flow that upon solidification forms a good weld between the plates. Typical values of different parameters for welding 1100 aluminum are: tool diameter = 6.25 mm, shoulder diameter = 19 mm, rotational speed = 700 rpm and translational speed = 3 mm/s. Alternatively, rotational speed of 1200 rpm coupled with translational speed of ~10 mm/s could be used. It was found that the weld process introduced extensive localized deformation near the boundaries of the molten material. Considerable heat is very likely produced during high speed machining wherein shear bands have been observed.

We note that deformations in all these processes are shear dominated with significant heat flux at the boundaries. Accordingly, we study simple shearing deformations of a thermo-elasto-viscoplastic material with both the tangential velocity and the heat flux prescribed at the boundaries to analyze localization of deformation near the boundaries. The prescribed heat flux at the boundaries makes the deformation inhomogeneous and introduces a nucleation site for the deformation to localize. The present work differs from the earlier ones in two respects: there is no artificial defect (such as a weak material, inhomogeneous initial temperature/porosity, non-uniform thickness of specimen) introduced to nucleate a shear band, and thermal energy is being continuously input into the body through the boundaries rather than the boundaries being thermally insulated. Thus heat conduction plays a noticeable role. The narrow region of intense plastic deformation, usually a few microns (μm) wide, is called a shear band.

It is generally believed that shear bands (SBs) were first observed by Tresca (1878) and subsequently by Massey (1928) during the hot forging of a bar. However, the research activity in this area picked up following their observation by Zener and Hollomon (1944) during the punching of a hole in a low-carbon steel plate. They also postulated that a material becomes unstable when its softening due to heating caused by plastic working overcomes its hardening due to strain and strain-rate effects. The SBs have been termed adiabatic since they form in a few micro-seconds after initiation and there is not enough time for the heat to be conducted away from them. Numerical simulations of problems with thermally insulated boundaries (e.g. see Batra and Kim (1991)) have revealed that heat conduction plays a negligible role till they initiate but plays a dominant role during their development and in the post-localization process. Marchand and Duffy (1988) tested thin-walled tubes in torsion and observed that the SB initiation was accompanied by a rapid drop in the torque required to deform the tube and hence in the shear stress in the shear-banded region. This occurred at a nominal shear strain much higher than that at which the shear stress peaked. These and other works on adiabatic SBs are summarized in two books

(Bai and Dodd (1992), Wright (2002)), special issues of three journals (e.g. see Armstrong et al. (1994), Zbib et al. (1992), Batra et al. (2000)), two volumes edited by Perzyna (1998), and Batra and Zbib (1994), review article of Tomita (1994) and the summary paper by Batra (1998). Furthermore, Batra (1987a) has characterized the effect of different material parameters on the initiation and development of SBs; Batra and Kim (1992), and Batra and Lear (2005) have ranked different materials according to their susceptibility to shear banding. Batra and Love (2004, 2005a) and Charalambakis and Baxevanis (2004) have analyzed the development of shear bands in non-homogeneous materials, and Batra and Zhu (1991) and Zhu and Batra (1991) have studied their initiation and propagation in a laminated body. For plane strain deformations of functionally graded materials comprised of tungsten particulates in nickel-iron matrix, Batra and Love (2005b) have delineated the initiation and propagation of a crack due to either a brittle or a ductile failure.

The paper is organized as follows. Section 2 describes the problem formulation. The computational procedure used to find a numerical solution of the problem and computed results are given in Section 3. Conclusions are summarized in Section 4.

2. Formulation of the problem

We study simple shearing deformations of a homogeneous and isotropic thermo-elasto-viscoplastic body occupying the domain $-H \leqslant y \leqslant H$ and sheared by equal and opposite tangential velocity V_0 prescribed on surfaces $y = \pm H$. Here, in addition to the velocity prescribed on $y = \pm H$, heat flux is also prescribed. Thus both mechanical and thermal energies are input into the body through the boundaries. Let the spatial coordinate be normalized by H, the shear stress by τ_0, time by H/V_0, and the temperature by θ_0. In terms of non-dimensional variables, the body occupies the domain bounded by the planes $y = \pm 1$. Henceforth, unless otherwise specified, we use non-dimensional variables. Equations governing dynamic finite thermomechanical deformations of the body are (e.g. see Batra (1987a,b))

$$
\begin{aligned}
&\rho \dot{v} = \tau_{,y}, \\
&\dot{\theta} = \lambda \theta_{,yy} + \tau \dot{\gamma}_{\mathrm{p}}, \\
&\dot{\gamma} = v_{,y} = \dot{\gamma}_{\mathrm{e}} + \dot{\gamma}_{\mathrm{p}}, \\
&\dot{\tau} = \mu \dot{\gamma}_{\mathrm{e}}, \\
&\dot{\gamma}_p = \dot{\gamma}_* \exp\left[\left(\frac{\tau}{(A + B\gamma_{\mathrm{p}}^n)(1 - \theta_*^m)} - 1\right)/C\right], \\
&\theta_* = \frac{\theta - \theta_{\mathrm{r}}}{\theta_{\mathrm{m}} - \theta_{\mathrm{r}}}.
\end{aligned}
\tag{1}
$$

For boundary conditions we take

$$
v(\pm 1, t) = \pm 1, \quad -\lambda \theta_{,y}(\pm 1, t) = q(t),
\tag{2}
$$

and for initial conditions,

$$\theta(y,0) = \theta_{\mathrm{r}}, \quad \gamma_{\mathrm{p}}(y,0) = 0, \quad \gamma(y,0) = 0, \quad v(y,0) = y, \quad \tau(y,0) = 1. \tag{3}$$

Here a superimposed dot indicates the material time derivative, a comma followed by y signifies partial differentiation with respect to y, ρ is the mass density, v the velocity, τ the shear stress, γ the shear strain, $\dot{\gamma}$ the shear strain rate, t the time, q the heat flux and θ the present temperature of a material particle. Furthermore, λ is the thermal diffusivity, and μ the shear modulus of the material. Eq. (1)$_1$ and (1)$_2$ express, respectively, the balance of linear momentum and the balance of internal energy. All of plastic working, given by the second term on the right-hand-side of Eq. (1)$_2$, is assumed to be converted into heating. Eq. (1)$_3$ is the definition of strain rate, and Eq. (1)$_4$ implies that the strain-rate has additive decomposition into elastic and plastic parts. Eq. (1)$_5$ is Hooke's law written in the rate form, and Eq. (1)$_6$ is the thermo-viscoplastic relation due to Johnson and Cook (1983). In it, $\dot{\gamma}_*$ is the reference strain rate, and θ_{m} and θ_{r} are the melting temperature and the reference temperature, respectively. The parameters m, n and C characterize, respectively, the thermal softening, strain hardening, and strain rate hardening characteristics of the material. All material parameters are presumed to be constants for the range of strains, strain-rates and temperatures anticipated to occur in this problem. We note that Johnson and Cook (1983) determined material parameters from torsional test data over a limited (low) range of strains, strain-rates, and temperatures. The range of strain rates and temperatures anticipated to occur within a shear band is considerably more than that used by Johnson and Cook. Also, for some materials, phase transitions and damage may occur within a SB. Thus, results presented herein are approximate, and help establish general trends.

The non-dimensional parameters are related to their dimensional (barred) counterparts as follows:

$$y = \bar{y}/H, \quad t = \bar{t}\dot{\gamma}_0, \quad \theta = \bar{\theta}\bar{\rho}\bar{c}/\bar{A}, \quad \lambda = \bar{k}/\bar{\rho}\bar{c}\dot{\gamma}_0 H^2, \ \rho = \bar{\rho}H^2\dot{\gamma}_0^2/\tau_0,$$
$$q = \bar{q}/\dot{\gamma}_0 H \tau_0. \tag{4}$$

Here c is the specific heat, k the thermal conductivity and $\dot{\gamma}_0 = V_0/H$ the nominal strain rate.

Because of symmetry/antisymmetry of deformations about $y = 0$, deformations of the material in the region $0 \leqslant y \leqslant 1$ are analyzed. On the surface $y = 0$, boundary conditions $v(0,t) = 0$, $\theta_{,y}(0,t) = 0$ are imposed. Thus the surface $y = 0$ is stationary and thermally insulated. On the surface $y = 1$, the tangential velocity and the heat flux are prescribed.

Initially the body is at a uniform temperature θ_{r}, and the time is reckoned from the instant when transients have died out and steady state has been reached. Thus at $t = 0$, we set the total strain and the plastic strain equal to zero and the shear stress equal to the quasistatic yield stress of the material.

3. Computation and discussion of results

In order to compute results, we set $H = 3.18$ mm, $V_0 = 4.77$ m/s. Hence, the block is sheared at a nominal strain-rate of 1500/s. Values of other parameters, taken either from Johnson and Cook (1983) or Batra and Kim (1992), are listed in Table 1. Thus the reference temperature $\theta_0 = \bar{A}/(\bar{\rho}\bar{c})$ equals 122 K. That is, values of temperature rise in K equal 122 times the non-dimensional values reported below. The room temperature θ_r is set equal to 300 K.

The aforestated problem is solved numerically by the finite element method (FEM); e.g., see Batra and Kim (1990a). A weak form of governing equations is derived by the Galerkin approximation. The result is a system of coupled non-linear ordinary differential equations which are integrated by using the subroutine LSODE (Livermore Solver for Ordinary Differential Equations) that can be downloaded from the internet. It adjusts the time step adaptively to compute the solution within the prescribed accuracy. While using LSODE we set $MF = 10$, $ATOL = 10^{-6}$, $RTOL = 10^{-6}$, where $ATOL$ and $RTOL$ control, respectively, the absolute and the relative tolerances in the solution.

The FE code of Batra and Kim (1990a) has been modified to incorporate the non-zero heat flux boundary condition at $y = 1$. The modification of the code was validated by finding the transient temperature field in a semi-infinite body $y \leqslant 1$ with the heat flux prescribed at $y = 1$, the semi-infinite body is modeled by assigning a very large value to H. The computed solution at points near $y = 1$ was found to match within 0.01% with the analytical solution of the problem given in Carlsaw and Jaeger (1986).

We used two FE meshes with coordinates of nodes given by either

$$y_n = \left(8\left(\frac{n-1}{300}\right)\right)^{0.6}, \quad 1 \leqslant n \leqslant 31,$$

$$y_n = \left(\frac{n-1}{300}\right)^{0.05}, \quad 31 \leqslant n \leqslant 301, \text{ or} \tag{5}$$

$$y_n = 1 - \left(\frac{301-n}{300}\right)^4, \quad n = 1, 2, \dots 301.$$

In each case, more nodes are concentrated near the boundary $y = 1$ where heat flux is prescribed. Numerical solutions computed with these two meshes were virtually identical with each other and their plots overlapped. Results given below are with the FE mesh obtained by using $(5)_1$.

Table 1
Material parameters used for 4340 steel

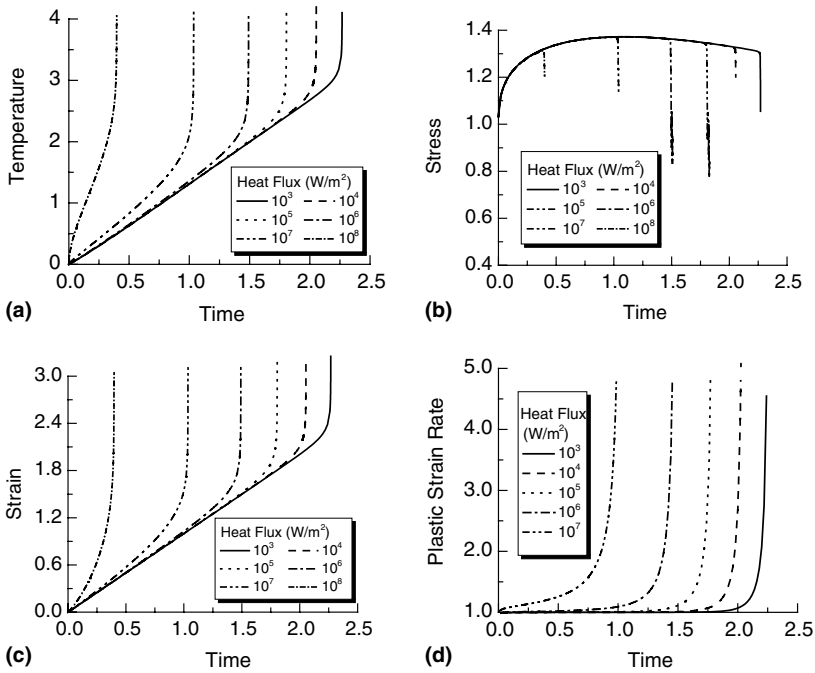| $\bar{\rho}$ (kg/m³)	$\bar{c}$ (J/kgK)	$\bar{\mu}$ (GPa)	$\bar{k}$ (W/mK)	θ_m (°C)	$\bar{A}$ (MPa)	$\bar{B}$ (MPa)	C	n	m	$\dot{\gamma}_*$ (1/s)
7840	477	76	38	1520	455	237	0.006	0.37	1.03	1

Fig. 1. For six values of the heat flux prescribed at $y = 1$, time histories of the evolution at $y = 1$ of (a) the temperature rise, (b) the shear stress, (c) the shear strain, and (d) the shear strain rate.

For six different values of the heat flux, Fig. 1(a)–(d) exhibits time histories of the non-dimensional temperature rise, the normalized shear stress, the shear strain and the non-dimensional plastic shear strain-rate at the point $y = 1$. Recalling that the temperature rise at a point on the top surface of a half space with prescribed heat flux $\bar{q}$ equals $\frac{2\bar{q}\bar{c}\bar{\rho}}{\bar{k}^{1/2}}(\frac{\bar{t}}{\pi})^{1/2}$ (e.g. see Carlsaw and Jaeger (1986)), it will take some time for the temperature to rise at the surface $y = 1$ and diffuse into rest of the specimen. With a rise in temperature of material points near $y = 1$, the shear stress needed to deform them plastically decreases and they deform more rapidly resulting in higher energy dissipation rate due to the internal shear stress. This further increases the temperature and in a way the process is self energizing. For thermally insulated boundaries, a state is reached when energy input through the working of externally applied traction at $y = 1$ equals that diffused through the boundary of a SB via heat conduction. Batra and Chen (2001) found that nearly 85% of the working of the tangential traction applied at $y = 1$ is conducted out of the boundary of the almost fully developed SB.

From the time history of the temperature rise plotted in Fig. 1a, we see that the initial rate of temperature increase varies with $\bar{q}$ but the explosive rate of temperature increase is virtually independent of $\bar{q}$. For every tenfold increase in the prescribed heat flux starting at 10^3 W/m^2, the difference in times for two successive values of the heat flux when the rapid drop in the shear stress and the simultaneous high

increase in the strain-rate occur becomes larger. For heat flux of 10^8 W/m^2 the shear stress drops before it attains its peak value. The temperature rise at the instant of the stress collapse decreases with an increase in $\bar{q}$; for $\bar{q} = 10^3$ W/m^2, $\Delta\theta \simeq 360$ K, and for $\bar{q} = 10^8$ W/m^2, $\Delta\theta \simeq 270$ K. One reason for this is that the stress drops sooner for $\bar{q} = 10^8$ W/m^2 than that for $\bar{q} = 10^3$ W/m^2. Since the tangential velocity prescribed at $y = 1$ is kept constant, therefore working of the shear traction applied at $y = 1$ is proportional to the shear stress at $y = 1$ and rapidly decreases once the deformation begins to localize there. The working due to applied tangential traction of 455 MPa equals 2.17×10^9 W/m^2. Thus prior to the beginning of the localization process, the working due to externally applied force exceeds the prescribed heat flux. It suggests that the prescribed heat flux of $\sim 10^6$ W/m^2 serves as a very weak defect and that of $\sim 10^8$ W/m^2 as a strong defect. However, once the deformation has begun to localize, the applied tangential traction (or the load required to deform the body) and hence the external working decrease. We note that the drop in the shear stress at $y = 1$ is accompanied by a sharp increase in the strain rate there signifying the strong thermal softening.
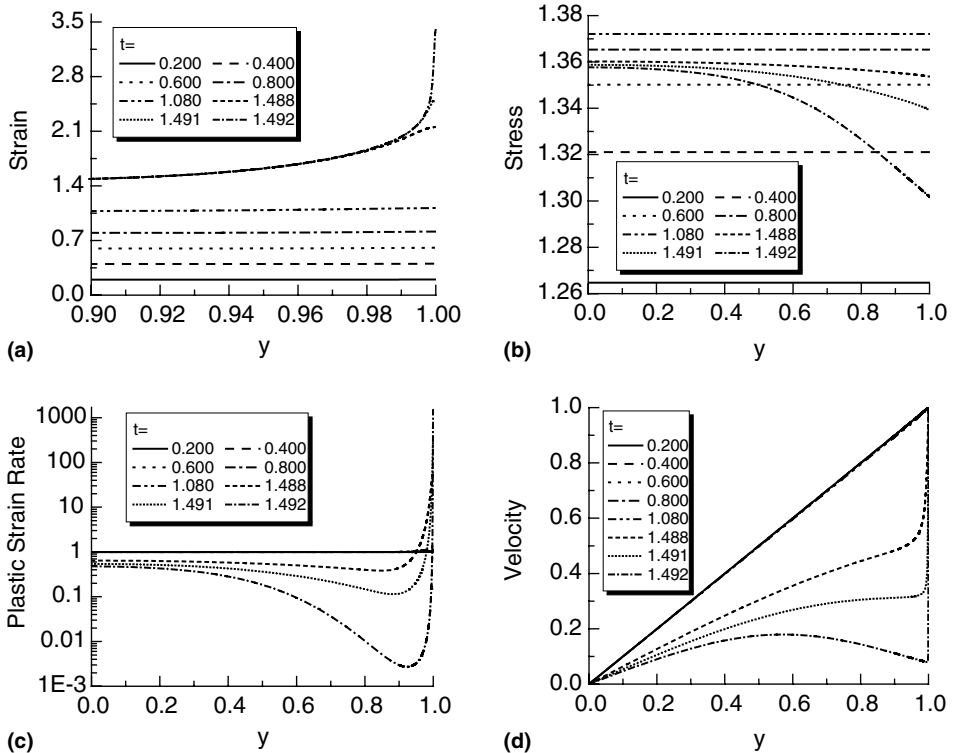

Fig. 2. For prescribed heat flux of 10^6 W/m^2 at $y = 1$, the spatial distribution at different times of: (a) the shear strain, (b) the shear stress, (c) the shear strain rate and (d) the velocity.

Initially the strain and strain-rate hardening effects exceed thermal softening and the shear stress required to maintain the prescribed average strain rate increases. As depicted in Fig. 2(a)–(b), the shear strain and the shear stress are essentially uniformly distributed in space with the shear stress at each material point rising in time till it peaks. Even though the temperature distribution (not shown) is non-uniform at all times with the highest temperature occurring at $y = 1$ and the lowest at $y = 0$, the shear stress is virtually constant throughout the region $0 \leqslant y \leqslant 1$. Because of the continuing rise in temperature difference between material points at $y = 1$ and those at $y < 1$ the shear stress at $y = 1$ peaks and subsequently drops rapidly. The non-dimensional time or the average shear strain when the shear stress at $y = 1$ peaks decreases with an increase in the value of $\bar{q}$; cf. Fig. 1(b). For $\bar{q} = 10^6$ W/m^2, the stress-drop at $y = 1$ occurs at $t \simeq 1$ ms. Note that as the shear stress at $y = 1$ begins to drop, the velocity field starts to deviate from the linear variation and a boundary layer develops near $y = 1$; e.g., see Fig. 2(d). At $t = 1.492$, the total strain rate or the velocity gradient derived from Fig. 2(d) is positive in the region $0 \leqslant y < {\sim}0.6$ but negative in the region ${\sim}0.6 < y < {\sim}0.98$. Since the plastic strain rate in the latter region (cf. Fig. 2(c)) has a small positive value, the elastic strain rate is negative in this region which contributes to the drop in the shear stress. Note that the total strain rate equals the sum of the elastic and the plastic strain rates. The positive value of the plastic strain rate implies that the yield stress, due to the rise in temperature, is decreasing at a rate faster than the rate of drop of the shear stress.

Batra and Kim (1992) numerically studied simple shearing deformations of twelve materials under thermally insulated boundary conditions but a geometric defect introduced at the block center to initiate a SB. They postulated that a SB initiates at a point when the shear stress there has dropped to 80% of its maximum value at that point and the material point is deforming plastically. This criterion has been successfully used in several subsequent numerical simulations of SBs performed under thermally insulated boundaries. In order to see if such a criterion can be used to delineate the initiation of a SB in the present problem, we have plotted in Fig. 3(a) and (b) the time history of the evolution of the plastic shear strain rate and the shear stress at $y = 1$ for $\bar{q} = 10^6$ W/m^2. Only the late time behavior is shown in this Figure. It is clear that for $t \geqslant 1.490 \simeq 1$ ms the shear strain rate oscillates even though the shear stress continues to drop monotonically first and then exhibits oscillations of very small amplitude. As $\bar{q}$ is increased from 10^3 to 25×10^7 W/m^2, the first peak in the strain rate at $y = 1$ has values decreasing from $1899\dot{\gamma}_0$ to $1075\dot{\gamma}_0$, where $\dot{\gamma}_0$ is the nominal strain-rate. We note that a similar oscillatory behavior occurs when the boundaries are thermally insulated, i.e., $\bar{q} = 0$; e.g., see Batra and Zhang (2004), Bayliss et al. (1994), Batra and Kim (1990a), and DiLellio and Olmstead (2003). These investigators employed different techniques to integrate the governing partial differential equations and is thus a characteristic of the governing equations and values assigned to material parameters. Batra and Kim (1990a) attributed these oscillations to the interplay between strain and strain-rate hardening and thermal softening. Once thermal softening becomes much larger than the hardening effects, the oscillations cease. For
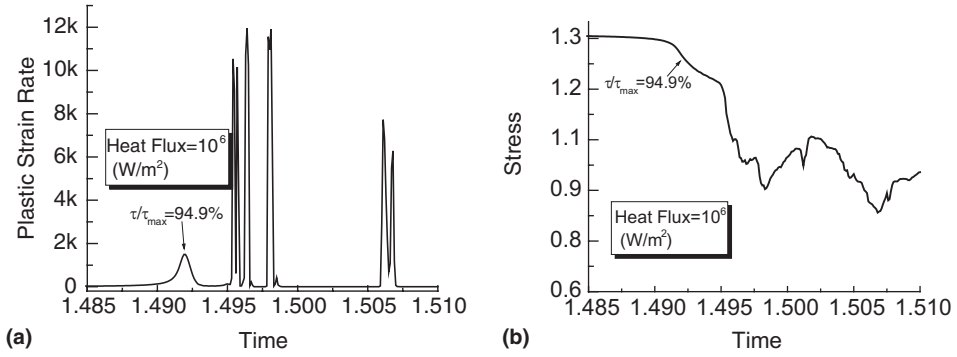
Fig. 3. For times near the ASB initiation, variation with time of: (a) the plastic strain-rate and (b) the shear stress at $y = 1$.

$\bar{q} = 10^6$ W/m^2, non-dimensional times corresponding to $\tau/\tau_{max} = 0.95$ and 0.8 at $y = 1$ are 1.492 and 1.496, respectively; these differ by less than 0.3%. With an increase in $\bar{q}$ from 10^4 W/m^2 to 10^8 W/m^2, τ/τ_{max} at the first peak in strain rate at $y = 1$ increases from 92.6% to 96.3%. To avoid the effect of oscillations in the strain rate at $y = 1$ on the SB initiation time, we hypothesize that a SB ensues at $y = 1$ when $\tau/\tau_{max} = 0.97$ there. This criterion is reasonable and is supported by experimental observations of Duffy and Chi (1992). They report that in torsional tests on thin-walled steel tubes a SB initiates soon after the shear stress attains its peak value.

The variations with the prescribed heat flux $\bar{q}$ of the SB initiation time, the temperature rise at the SB center and the localization ratio are depicted in Fig. 4(a)–(c); note the logarithmic scale along the horizontal axis. The localization ratio equals the shear strain at the band center divided by the nominal shear strain in the specimen and is a measure of the intensity of localization of deformation. For thermally insulated boundaries, Batra and Kim (1992) plotted the localization ratio for twelve materials. It is clear that with an increase in $\bar{q}$ the SB initiation time decreases rapidly, the temperature at the SB center increases monotonically, and the localization ratio increases. The intensity of localization for $\bar{q} = 10^8$ W/m^2 is nearly 10 times that for $\bar{q} = 10^2$ W/m^2. A least squares fit of a quadratic polynomial to the SB initiation time, t_{SB}, vs. $\log \bar{q}$ is

$$t_{SB} = 1.19 + 0.169(\log \bar{q}) - 0.0344(\log \bar{q})^2, \tag{6}$$

where t_{SB} is in ms, and $\bar{q}$ in W/m^2. Eq. (6) is valid for $10^3 \leqslant \bar{q} \leqslant 10^8$ W/m^2. We note that Molinari and Clifton (1987) and Duffy and Chi (1992) also predicted a logarithmic dependence on the defect size for the strain at localization. Neither results reported in Fig. 4 nor Eq. (6) are valid for $\bar{q} < 10^3$ W/m^2. For small values of $\bar{q}$, t_{SB} will increase exponentially approaching ∞ as $\bar{q}$ goes to zero. For $\bar{q} = 0$, deformations stay homogeneous and no SB forms.
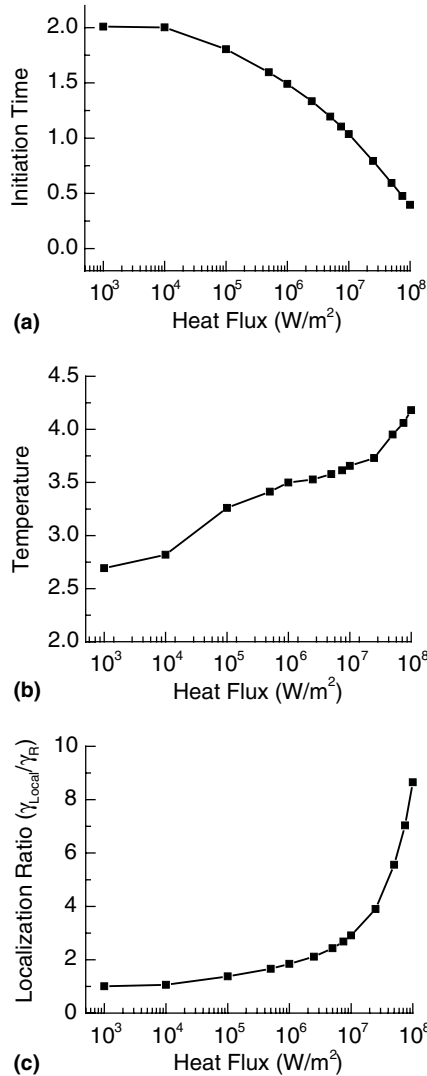
Fig. 4. Variation with the heat flux prescribed at $y = 1$ of: (a) the SB initiation time, (b) the temperature at the SB center, and (c) the localization ratio.

Marchand and Duffy (1988) defined the SB width as the width of the region over which the maximum plastic strain is constant. The band width is measured from post-mortem pictures of grid lines drawn on the unstressed specimen's outer surface. The level of maximum plastic strain within a SB depends upon the applied load and its duration. In numerical simulations, the band width computed according to this criterion will be zero since the maximum plastic strain occurs at one point only. Accordingly, Batra and Kim (1992) defined the band width as the width of the region

surrounding the band center over which the plastic strain differs from its peak value by less than 10%. Since the plastic strain at the band center continues to grow, the band width will vary with time. For thermally insulated boundaries driven at a uniform velocity, the SB width is determined by the diffusion through heat conduction of the plastic working within the shear banded region. For example, Batra and Chen (2001) found that 85% of plastic working is conducted through the boundaries of a nearly fully developed SB. For the present problem, with the thermal energy being continuously input at a uniform rate through the boundary at $y = 1$, both the energy input through the boundary $y = 1$ and that generated due to plastic working need to be conducted out of the SB boundaries for the SB width to attain a steady value. As vividly shown in Fig. 8 of Batra and Kim (1992) the computed band width varies with the localization ratio, and the half band width does not equal the distance from the center to the farthest point where the SB has initiated.

For $\bar{q} = 10^6$ W/m^2 and five values of t close to t_{SB} Fig. 5 exhibits the development of the shear strain at points near $y = 1$. It is evident that the intensely deformed region continues to shrink. If pictures of the deformed specimen were taken at $t = 1.492$, then the shear band width would equal $2 \times 0.001 \times 3.18$ mm = 6.36 μm.

For $\bar{q} = 10^6$ W/m^2, Fig. 6(a)–(d) evinces at the point $y = 1$ the time-histories of the evolution of the normalized shear stress, the shear strain, the non-dimensional plastic shear strain-rate and the non-dimensional temperature for several values of the nominal strain rate $\dot{\gamma}_0$. The results are qualitatively similar to those obtained earlier (e.g. see Batra (1988)) with thermally insulated boundaries. The nominal strain, but not the dimensional time, at which a SB initiates increases with an increase in the nominal strain rate. For example, the nominal strain or the non-dimensional times at the initiation of a SB at nominal strain rates of 10^2/s and 10^5/s equal ~1.2 and 1.8, respectively. However, the corresponding dimensional times are 12 and 0.018 ms. The localization ratio decreases with an increase in the nominal strain rate. A least squares fit to the computed values of t_{SB} for different values of $\dot{\gamma}_0$ is
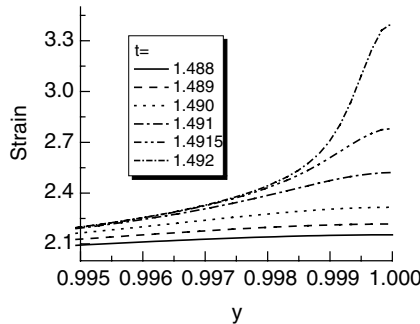

Fig. 5. At different times, variation of the shear strain at points close to the boundary $y = 1$, where heat flux is prescribed at 10^6 W/m^2.
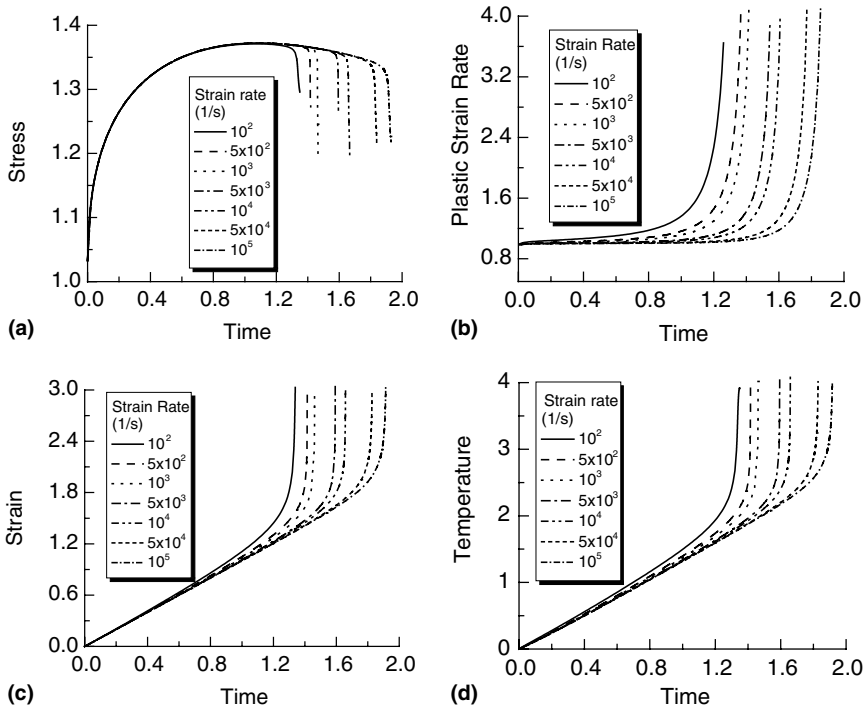
Fig. 6. For $\bar{q} = 10^6$ W/m^2, and several values of the nominal strain-rate, time histories at the point $y = 1$ of the evolution of: (a) the shear stress, (b) the strain-rate, (c) the strain, and (d) the temperature.

$$t_{SB} = [0.8112 + 0.00274 \log \dot{\gamma}_0 + 0.01747(\log \dot{\gamma}_0)^2], \tag{7}$$

where t_{SB} is in ms, $\dot{\gamma}_0$ is in 1/s, and $10^2/\text{s} \leqslant \dot{\gamma}_0 \leqslant 10^5/\text{s}$.

Here we have employed the Johnson and Cook (1983) relation to describe the thermo-viscoplastic response of the material. Batra and Kim (1990b), Batra and Jaber (2001), Batra and Chen (2001) and Batra and Jayachandran (1992) have shown that other viscoplastic relations give qualitatively similar but quantitatively different results. Batra and Chen (1999) and Daridon et al. (2004) have studied shear band spacing with different constitutive relations. Recently Batra and Wei (2005) have given a closed-form expression for shear band spacing in strain-hardening thermo-viscoplastic solids.

The length of the smallest element for the FE meshes given by Eq. (5)$_1$ and (5)$_2$ equal 0.53 μm and 4×10^{-7} μm, respectively. These and other similar FE meshes gave virtually identical values of the SB initiation time and width. For our problem, thermal conductivity controls the SB width; e.g. see Batra and Kim (1991). For locally adiabatic deformations the shear band width will equal the size of the smallest element in the FE mesh. For two- and three-dimensional problems one can not use such fine meshes. One way to obtain mesh-independent

results is to use a strain-rate gradient-dependent theory, e.g. see Batra (1987a,b), Batra and Kim (1990b) and Batra and Hwang (1994). Such theories involve a material characteristic length and third-order spatial gradients of displacements or velocities in the problem formulation thereby necessitating the use of either Hermitian basis functions or auxiliary variables. At present, to our knowledge, there are no good ways of estimating the material characteristic length. Furthermore, these theories may either not give a finite speed of elastic waves or a unique solution of the linear elastic problem; see Batra (1975) for the corresponding thermal problem. Batra and Chen (1999), and Chen and Batra (1999) employed a strain-rate-gradient dependent plasticity theory to find spacing between adjacent SBs. Alternatively, one can use an adaptively refined mesh to delineate the width of a SB; e.g. see Batra and Ko (1992, 1993) and Batra and Hwang (1993). Frequent remeshing smoothens out the deformation fields and consequently delays the initiation of an ASB. Another possibility is to use a meshless method such as the modified smoothed particle hydrodynamics method (e.g. see Batra and Zhang (2004)).

4. Conclusions

We have analyzed simple shearing deformations of a thermo-elasto-viscoplastic body deformed at a prescribed nominal strain rate and with a constant heat flux input through its boundaries. The initial state of the body corresponds to a uniform state of deformation. The deformation localizes near the boundaries where the heat flux is prescribed. The rate of deformation localization, i.e., the reciprocal of the time required to form a shear band, increases rapidly with an increase in the value of the prescribed heat flux. The time of initiation of a shear band depends upon the logarithm of the heat flux and the logarithm of the nominal strain rate. The width of the intensely deformed region continues to decrease with time because of the constant heat input through the boundaries. Whereas for thermally insulated boundaries the shear band initiation time is determined by when and how large a perturbation is introduced to disturb the homogeneous solution, here it is ascertained by the heat flux prescribed at the boundaries. The major quantitative differences in the two cases are in the time of initiation of a SB and in its width. For thermally insulated boundaries, these are determined by the size and the type of the initial defect, for the present problem they are determined by the heat flux prescribed at the boundaries which may be viewed as a defect.

References

Armstrong, R., Batra, R.C., Meyers, M., Wright, T.W. (Eds.), 1994. Shear Instabilities and Viscoplasticity Theories, a Special Issue of the Mechs. of Materials, vol. 17, pp. 83–328.

Aukrust, T., Lazghab, S., 2000. Thin shear boundary layers in flow of hot aluminum. Int. J. Plasticity 16, 59–71.

Bai, Y., Dodd, B., 1992. Adiabatic Shear Localization-Occurrence, Theories and Applications. Pergamon Press.

Batra, R.C., 1975. On heat conduction and wave propagation in non-simple rigid solids. Lett. Appl. Eng. Sci. 3, 97–107.

Batra, R.C., 1987a. Effect of material parameters on the initiation and growth of adiabatic shear bands. Int. J. Solids Struct. 23, 1435–1446.

Batra, R.C., 1987b. The initiation and growth of, and the interaction among adiabatic shear bands in simple and dipolar materials. Int. J. Plasticity 3, 75–89.

Batra, R.C., 1988. Effect of nominal strain-rate on the initiation and growth of adiabatic shear bands in steels. J. Appl. Mech. 55, 229–230.

Batra, R.C., 1998. Numerical solution of initial-boundary-value problems with shear strain localization. In: Perzyna, P. (Ed.), Localization and Fracture Phenomenon in Inelastic Solids. Springer-Verlag, Wien, pp. 301–389.

Batra, R.C., Chen, L., 1999. Shear band spacing in gradient-dependent thermoviscoplastic materials. Comput. Mech. 23, 8–19.

Batra, R.C., Chen, L., 2001. Effect of viscoplastic relations on the instability strain, shear band initiation strain, the strain corresponding to the maximum shear band spacing, and the band width in a thermoviscoplastic material. Int. J. Plasticity 17, 1465–1489.

Batra, R.C., Hwang, J., 1993. An adaptive mesh refinement technique for two-dimensional shear band problems. Comput. Mech. 12, 255–268.

Batra, R.C., Hwang, J., 1994. Dynamic shear band development in dipolar thermoviscoplastic materials. Comput. Mech. 12, 354–369.

Batra, R.C., Jaber, N.A., 2001. Failure mode transition in an impact loaded prenotched plate with four thermoviscoplastic relations. Int. J. Fracture 110, 47–71.

Batra, R.C., Jayachandran, R., 1992. Effect of constitutive models on steady state axisymmetric deformations of thermoelastic–viscoplastic targets. Int. J. Impact Eng. 12, 209–226.

Batra, R.C., Kim, C.H., 1990a. Adiabatic shear banding in elastic–viscoplastic nonpolar and dipolar materials. Int. J. Plasticity 6, 127–141.

Batra, R.C., Kim, K.H., 1990b. Effect of viscoplastic flow rules on the initiation and growth of shear bands at high strain rates. J. Mech. Phys. Solids 38, 859–874.

Batra, R.C., Kim, C.H., 1991. Effect of thermal conductivity on the initiation and growth of adiabatic shear bands in steels. Int. J. Eng. Sci. 29, 949–960.

Batra, R.C., Kim, C.H., 1992. Analysis of shear banding in twelve materials. Int. J. Plasticity 8, 425–452.

Batra, R.C., Ko, K.I., 1992. An adaptive mesh refinement technique for the analysis of shear bands in plane strain compression of a thermoviscoplastic solid. Comput. Mech. 10, 369–379.

Batra, R.C., Ko, K.I., 1993. Analysis of shear bands in dynamic axisymmetric compression of a thermoviscoplastic cylinder. Int. J. Eng. Sci. 31, 529–547.

Batra, R.C., Lear, M.H., 2005. Adiabatic shear banding in plane strain tensile deformations of eleven thermoelastoviscoplastic materials with finite thermal wave speed. Int. J. Plasticity 21, 1521–1545.

Batra, R.C., Love, B.M., 2004. Adiabatic shear bands in functionally graded materials. J. Therm. Stresses 27, 1101–1123.

Batra, R.C., Love, B.M., 2005a. Mesoscale analysis of shear bands in high strain sate deformations of tungsten/nickel-iron composites. J. Thermal Stresses 28 (in press).

Batra, R.C., Love, B.M., 2005b. Crack propagation due to brittle and ductile failures in microporous thermoelastoviscoplastic functionally graded materials. Eng. Fract. Mech. (accepted).

Batra, R.C., Rajapakse, Y.D.S., Rosakis, A., 2000. Failure mode transitions under dynamic loading. Int. J. Fracture 101, 1–180 (special issue).

Batra, R.C., Wei, Z.G., 2005. Shear band spacing in thermoviscoplastic materials. Int. J. Impact Eng. (accepted).

Batra, R.C., Zbib, H.M., 1994. Material Instabilities: Theory and Applications. ASME Press.

Batra, R.C., Zhang, G.M., 2004. Analysis of adiabatic shear bands in elasto-thermo-viscoplastic materials by modified smoothed particle hydrodynamics (MSPH) method. J. Comput. Phys. 201, 172–190.

Batra, R.C., Zhu, Z.G., 1991. Dynamic adiabatic shear band development in a bimetallic body containing a void. Int. J. Solids Struct. 27, 1829–1854.

Bayliss, A., Belytschko, T., Kulkarni, M., Lott-Crumpler, D.A., 1994. On the dynamics and the role of imperfections for localization in thermo-viscoplastic materials. Model. Simul. Mat. Sci. Eng. 2, 941–964.

Carlsaw, H.S., Jaeger, J.C., 1986. Conduction of Heat in Solids, second ed. Oxford University Press, Oxford.

Charalambakis, N., Baxevanis, T., 2004. Adiabatic shearing of non-homogeneous thermoviscoplastic materials. Int. J. Plasticity 20, 899–914.

Chen, L., Batra, R.C., 1999. Effect of material parameters on shear band spacing in work-hardening gradient-dependent thermoviscoplastic materials. Int. J. Plasticity 15, 551–574.

Daridon, L., Oussouaddi, O., Ahzi, S., 2004. Influence of the material constitutive models on the adiabatic shear band spacing: MTS, power law and Johnson–Cook models, Int. J. Solids Struct. 41, 3109–3124.

DiLellio, J.A., Olmstead, W.E., 2003. Numerical solution of shear localization in Johnson–Cook materials. Mech. Mater. 35, 571–580.

Duffy, J., Chi, Y.C., 1992. On the measurement of local strain and temperature during the formation of adiabatic shear bands. Mater. Sci. Eng. A 157, 95–210.

Johnson, G.R., Cook, W.H., 1983. A constitutive model and data for metals subjected to large strains, high strain-rates, and high temperatures. In: Proceedings of the 7th International Symposium on Ballistics, pp. 541–547.

Marchand, A., Duffy, J., 1988. An experimental study of the deformation process of adiabatic shear bands in a structural steel. J. Mech. Phys. Solids 36, 251–283.

Massey, H.F., 1928. The flow of metal during forging. Proc. Manchester Assoc. Eng., 21–26.

Molinari, A., Clifton, R.J., 1987. Analytical characterization of shear localization in thermoviscoplastic materials. J. Appl. Mech. 54, 806–812.

Moss, G.L., 1981. Shear strains, strain rates, temperature changes in adiabatic shear bands. In: Meyers, L.E., Murr, L.E. (Eds.), Shock Waves and High Strain Rate Phenomena in Metals. Plenum Press, New York, pp. 299–312.

Perzyna, P. (Ed.), 1998. Localization and Fracture Phenomenon in Inelastic Solids. Springer-Verlag, Wien, New York.

Schneider, J.A., Nunes Jr., A.C., 2004. Characterization of plastic flow and resulting microtextures in a friction stir weld. Metall. Mater. Trans. B 35, 777–783.

Seidel, T.U., Reynolds, A.P., 2001. Visualization of the material flow in AA2195 friction stir welds using a marker insert technique. Metall. Mater. Trans. 32A, 2879–2884.

Tomita, Y., 1994. Simulation of plastic instabilities in solid mechanics. Appl. Mech. Rev. 47, 171–205.

Tresca, K., 1878. On further application of flow of solids. Proc. Inst. Mech. Eng. 30, 301–345.

Wright, T.W., 2002. The Physics and Mathematics of Adiabatic Shear Bands. Cambridge University Press, Cambridge.

Zbib, H.M., Shawki T., Batra, R.C. (Eds.), 1992. Material Instabilities. Appl. Mech. Rev. 45, 1–173 (special issue).

Zener, C., Hollomon, J.H., 1944. Effect of strain rate upon plastic flow of steel. J. Appl. Phys. 15, 22–32.

Zhu, Z.G., Batra, R.C., 1991. Analysis of shear banding in plane strain compression of bimetallic thermally softening viscoplastic body containing an elliptical void. J. Eng. Mater. Technol. 113, 382–395.